

Reduced Plasma Kallistatin Is Associated With the Severity of Coronary Artery Disease, and Kallistatin Treatment Attenuates Atherosclerotic Plaque Formation in Mice

Yuyu Yao, PhD; Bing Li, MD; Chang Liu, MD; Cong Fu, MD; Pengfei Li, PhD; Youming Guo, PhD; Genshan Ma, MD; Naifeng Liu, MD; Lee Chao, PhD; Julie Chao, PhD

Background—Kallistatin exerts beneficial effects on organ injury by inhibiting oxidative stress and inflammation. However, the role of kallistatin in atherosclerosis is largely unknown. Here, we investigated the role and mechanisms of kallistatin in patients with coronary artery disease (CAD), atherosclerotic plaques of apoE^{-/-} mice, and endothelial activation.

Methods and Results—Plasma kallistatin levels were analyzed in 453 patients at different stages of CAD. Kallistatin levels were significantly lower in patients with CAD and negatively associated with CAD severity and oxidative stress. Human kallistatin cDNA in an adenoviral vector was injected intravenously into apoE^{-/-} mice after partial carotid ligation, with or without nitric oxide synthase inhibitor (N^o-nitro-L-arginine methyl ester) or sirtuin 1 inhibitor (nicotinamide). Kallistatin gene delivery significantly reduced macrophage deposition, oxidative stress, and plaque volume in the carotid artery, compared with control adenoviral injection. Kallistatin administration increased endothelial nitrous oxide synthase, sirtuin 1, interleukin-10, superoxide dismutase 2, and catalase expression in carotid plaques. The beneficial effects of kallistatin in mice were mitigated by N^o-nitro-L-arginine methyl ester or nicotinamide. Furthermore, human kallistatin protein suppressed tumor necrosis factor- α -induced NADPH oxidase activity and increased endothelial nitrous oxide synthase and sirtuin 1 expression in cultured human endothelial cells. These effects were also abolished by N^o-nitro-L-arginine methyl ester or nicotinamide.

Conclusions—This was the first study to demonstrate that reduced plasma kallistatin levels in patients are associated with CAD severity and oxidative stress. Kallistatin treatment prevents carotid atherosclerotic plaque formation in mice by stimulating the sirtuin 1/endothelial nitrous oxide synthase pathway. These findings indicate the potential protective effects of kallistatin on atherosclerosis in human subjects and mouse models. (*J Am Heart Assoc.* 2018;7:e009562. DOI: 10.1161/JAHA.118.009562)

Key Words: atherosclerosis • coronary artery disease • kallistatin • oxidative stress • sirtuin 1

Cardiovascular disease remains the primary cause of death worldwide.^{1,2} Atherosclerosis is the most common cause of cardiovascular disease.³ Numerous experimental and clinical studies have demonstrated that hypercholesterolemia, hypertension, diabetes mellitus, and smoking are traditional risk factors for atherosclerosis.⁴ Oxidative stress production from these risk factors is a major

cause of endothelial dysfunction, which is a crucial form of damage in the pathogenesis of atherosclerosis that contributes to plaque initiation and progression.⁵ Additionally, excess production of oxidative stress plays a vital role in vascular inflammation and leads to infiltration of monocytes/macrophages in the plaque.⁶ Many studies support the fact that antioxidants have therapeutic benefits in the fight against cardiovascular disease progression, but clinical trials have failed to show these benefits⁷; thus, more definitive and specific investigations are required. In addition, a better understanding of the complexity of oxidative stress in vascular biology may lead to more effective therapeutic strategies.

As an endogenous protein, kallistatin has been shown to regulate multiple signaling pathways and cell functions.⁸ Previous studies have demonstrated that kallistatin is involved in the regulation of vascular biological responses through its anti-inflammatory, antiangiogenic, and antioxidative properties.⁹⁻¹¹ The protective effects of kallistatin on the heart and kidney are associated with reduced oxidative

From the Department of Cardiology, Zhongda Hospital, Medical School of Southeast University, Nanjing, China (Y.Y., B.L., C.L., C.F., G.M., N.L.); Department of Biochemistry and Molecular Biology, Medical University of South Carolina, Charleston, SC (P.L., Y.G., L.C., J.C.).

Correspondence to: Yuyu Yao, PhD, Department of Cardiology, Zhongda Hospital, Southeast University, 87 Dingjiaqiao, Nanjing, Jiangsu 210009, China. E-mail: yaoyuyunj@hotmail.com

Received April 20, 2018; accepted October 10, 2018.

© 2018 The Authors. Published on behalf of the American Heart Association, Inc., by Wiley. This is an open access article under the terms of the Creative Commons Attribution-NonCommercial License, which permits use, distribution and reproduction in any medium, provided the original work is properly cited and is not used for commercial purposes.

Clinical Perspective

What Is New?

- An important finding is that plasma kallistatin levels were significantly lower in patients with coronary artery disease and that plasma kallistatin was negatively associated with oxidative stress and coronary artery disease severity.
- Kallistatin administration inhibited plaque formation by activating the sitruin1/endothelial nitrous oxide synthase pathway and inhibiting oxidative stress.

What Are the Clinical Implications?

- The findings suggest a role for kallistatin in the pathophysiology of atherosclerosis.
- Upregulation of kallistatin is a potential therapeutic strategy for the treatment of vascular diseases in the future.

stress and increased NO levels.^{12,13} Although many of the antioxidative stress and anti-inflammatory functions of kallistatin have been studied in recent years, the role of kallistatin in atherosclerosis remains unknown. Due to the important roles of inflammation and oxidative stress in all phases of atherosclerosis development, uncovering the role of kallistatin in atherosclerosis will not only shed a different light on the function of kallistatin but also help us understand the pathogenesis of atherosclerosis.

In this study we hypothesized that kallistatin plays an important role in maintaining vascular homeostasis, which has antiatherosclerotic effects, and that its circulating levels are decreased in patients with coronary artery disease (CAD). This study was designed to evaluate the relationship between plasma levels of kallistatin and CAD patients. Here, we measured the oxidative stress biomarker malondialdehyde (MDA) for comparison. To clarify the biological functions of kallistatin and its relation to atherosclerosis, apoE^{-/-} carotid partial ligation model mice fed a high-fat diet were injected via the tail vein with either adenovirus containing null cDNA (Ad.Null) or adenovirus carrying the human kallistatin cDNA (Ad.HKS). We therefore examined the influence of human kallistatin on low-shear stress-induced atherosclerosis in mice. We also explored the mechanism of kallistatin on tumor necrosis factor (TNF)- α -induced effects in cultured endothelial cells.

Materials and Methods

The data, analytic methods, and study materials will be made available on request to other researchers for the purposes of reproducing the results or replicating the procedure.

Ethics Committee Approval

Each patient gave written informed consent, and the study protocol was approved by the Ethics Committee of Southeast University Affiliated Zhongda Hospital and complied with the Declaration of Helsinki. All animal procedures were based on the National Institutes of Health guidelines for the use of live animals and were approved by the Medicine Animal Welfare Committee of the Medical School of Southeast University (Nanjing, China).

Study Population

This is a retrospective study on consecutive patients who had received first-time coronary angiography for diagnostic purposes between September 2015 and December 2015. After the initial screening, according to coronary angiography results and based on inclusive and exclusive criteria, 321 inpatients with newly diagnosed CAD and 132 CAD-free controls (normal coronary angiography or less than a 30% stenosis) were enrolled in the study.

Subjects with the following conditions were excluded: acute coronary syndromes or recent myocardial infarction (<3 months), hepatic or renal dysfunction, active infections or inflammatory conditions, previous coronary bypass surgery or percutaneous coronary intervention, congestive heart failure (New York Heart Association Class III, IV), a history of malignancy, recent trauma or surgery, or any type of immune-mediated disease. All subjects underwent quantitative coronary angiography with a cardiovascular measurement system Angiostar plus (Siemens, Munich, Germany) shortly after being admitted to the hospital. We categorized 321 patients as having “significant CAD” (luminal diameter narrowing $\geq 50\%$, a severity level previously correlated with reduced coronary flow reserve according to the clinical standards of the American College of Cardiology/American Heart Association guidelines for coronary angiography). Patients with CAD were further classified according to the number of diseased coronary arteries (1-, 2-, or 3-vessel disease). The severity of CAD on the angiogram was expressed as the sum of the Gensini scores for each lesion, which are calculated based on the number of stenotic segments and their respective degrees of luminal narrowing and localization within all 3 coronary arteries.¹⁴ The control group consisted of 132 subjects with either normal coronary arteries or nonsignificant CAD. Two investigators blinded to the clinical data of patients analyzed the results of the coronary angiogram. We collected the medication history of control and CAD patients.

Biochemical Assessment

Blood samples were collected from subjects before coronary angiography. Plasma was obtained from EDTA-treated

peripheral blood samples centrifuged at 2000g for 10 minutes and stored at -70°C until further analysis. All other standard hematological and biochemical analyses were routinely performed in the hospital laboratory.

The concentration of plasma MDA, which reflects oxidative stress, was determined by the spectrophotometric method based on the reaction between MDA and thiobarbituric acid. An MDA assay kit (Nanjing Jiancheng Bioengineering Institute, Nanjing, Jiangsu, China) was used to determine the degree of *in vivo* oxidative stress in 453 patients with CAD and controls.

Human kallistatin levels in plasma were determined using an ELISA specific for human kallistatin as previously described.¹⁵

Animal Models

Low-Shear Stress Induces Atherosclerotic Plaques in Mice

All surgeries were performed under anesthesia with sodium pentobarbital (50 mg/kg, intraperitoneal), and efforts were made to minimize animal suffering. Twelve-week-old male apoE^{-/-} mice (n=40) were obtained from the Changzhou Cavens Laboratory Animal Co, Ltd (Changzhou, China). The animals were fed a Western-type diet for 2 weeks before surgery. In all animals, the left external and internal carotid arterial branches were isolated and ligated with 6-0 silk sutures as previously described.¹⁶ One hour after surgery, mice that underwent partial ligation were randomly administered a tail vein injection of Ad.Null or Ad.HKS in a total volume of 200 μL (2×10^9 plaque-forming units in PBS). Those mice were divided into 4 groups (n=10 mice per group): Ad.Null, Ad.HKS, or Ad.HKS+N^ω-nitro-L-arginine methyl ester (L-NAME) 1 mg/mL (Sigma-Aldrich, St. Louis, MO) was dissolved in water and added directly to the drinking water of the animals, or Ad.HKS+sirtuin 1 (SIRT1) inhibitor nicotinamide (NAM); 10 mg/kg by intraperitoneal injection. L-NAME was used to assess the influence of NO on the protective effect of kallistatin, and NAM was used to assess the influence of SIRT1 on the protective effect of kallistatin. Two weeks later, magnetic resonance imaging (MRI) scans were performed to measure the carotid diameter and plaque volume in all animals, and human kallistatin levels in mouse plasma after gene delivery were determined by ELISA. In addition, plasma MDA levels were determined using an MDA assay kit (Nanjing Jiancheng Bioengineering Institute, Nanjing, Jiangsu, China). Plasma samples were used for the analysis of TNF- α using a Mouse TNF- α ELISA (Proteintech, Rosemount, IL) according to the manufacturer's protocol.

In Vivo MRI

All MRI scans were conducted with a micro-MR animal scanner (7.0T Bruker PharmaScans, Germany) as previously

described.¹⁶ Continuous MRI slices allowed the measurement of vascular intima and adventitia diameters and areas using semiautomated computer-assisted quantitative image analysis. Furthermore, we calculated plaque volume by summing the plaque areas for each slice and then multiplying the resulting value by the slice thickness.

Morphological Examination and Immunohistochemistry

At the end of the procedure, the mice were euthanized in a CO₂ chamber. Then, carotid arteries were excised and immediately embedded in Tissue-Tek OCT compound (Sakura Finetek Japan Co, Tokyo, Japan; n=5/group). Serial cryosections were cut on a Leica Cryostat (Wetzlar, Germany) and stained routinely with hematoxylin and eosin and oil red O. Superoxide levels in carotid artery plaque were determined by the fluorescent probe dihydroethidium.¹¹ Briefly, carotid artery plaque ring segments (7 μm thick) were stained with 2 $\mu\text{mol/L}$ dihydroethidium in a light-protected humidified chamber at 37 $^{\circ}\text{C}$ for 30 minutes. Images were obtained with a fluorescence microscope (Olympus CK40, Tokyo, Japan). The intensity of the fluorescence signal was quantitated using ImageJ software (National Institutes of Health, Bethesda, MD). Five mice per group were analyzed. The presence of CD68 (AbD Serotec, Bio-Rad, Hercules, CA) staining was used to detect macrophages. At least 5 sections were stained per mouse, and quantification was performed in a blinded manner. TNF- α expression was stained with antibody against TNF- α from Abcam (Cambridge, MA) using a standard 3-step biotin-streptavidin-peroxidase immunostain. Carotid arteries were collected in C57BL/6 and apoE^{-/-} mice. Cryosections 7 μm thick were subjected to immunohistochemical analysis to detect the presence of the endogenous mouse kallistatin (Sino Biological, Beijing, China). Endothelial nitric oxide synthase (eNOS) (Cell Signaling Technology, Danvers, MA)/CD31 and SIRT1 (Santa Cruz Biotechnology, Dallas, TX)/CD31 double staining was used to detect eNOS/endothelium and SIRT1/endothelium colocalization, respectively.

Quantitative Real-Time PCR

Because the left carotid artery plaque area is very small, we extracted RNA from half of the mice per group (n=5/group). Total RNA was extracted from the left carotid artery plaque area using TRIzol reagent (Invitrogen, Carlsbad, CA). cDNA was transcribed using a cDNA archive kit (Gene Amp PCR System 9700, Applied Biosystems, Foster City, CA). Quantitative real-time polymerase chain reaction (PCR) was carried out using a SYBR Green PCR master mix kit and a ViiA 7 Real-time PCR system (Applied Biosystems, Foster City, CA).

Transcription of the housekeeping gene β -actin was determined by a specific primer/probe mix (Applied Biosystems). The final quantification was performed using Relative Quantification software (Applied Biosystems). A list of all the primers used is provided in Table 1.

Total RNA was isolated from cultured cells (see below) with TRIzol reagent (Invitrogen, Carlsbad, CA) following the manufacturer's protocol. Total RNA was reverse-transcribed using the High-Capacity cDNA Reverse Transcription Kit. Real-time PCR was performed with the TaqMan Gene Expression Assay using an ABI 7300 real-time PCR system (Applied Biosystems). The primers Hs01009003_m1 and Hs00167166_ml were used for the detection of SIRT1 and eNOS expression, respectively, and 18S (Hs99999901_s1) was used as an internal control.

Endothelial Cell Culture

Primary human umbilical vein endothelial cells used in these studies were maintained at 37°C under 5% CO₂ in Essential Cell Growth Medium (Clonetics, Cambrex Corporation, East Rutherford, NJ). Passages 3 and 4 were used in this study. Human umbilical vein endothelial cells were preincubated with human kallistatin¹⁷ (1 μ mol/L) for 30 minutes and then stimulated with TNF- α (15 ng/mL) for an additional 18 hours. To determine the role of the SIRT1/eNOS pathway, inhibitors against eNOS (L-NAME, 100 μ mol/L) and SIRT1 (NAM, 5 mmol/L) were added 30 minutes before kallistatin treatment.

Table 1. Primers With Forward and Reverse Sequences Used in qPCR

Target Gene	Prime Sequences	Annealing (°C)	Amplicon Size (bp)
β -actin	F:5' GTACCACCATGTACCCAGGC3' R :5'AACGCAGCTCAGTAACAGTCC3'	60	247
eNOS	F:5'CTGGCAAGACAGACTACACGAC3' R:5'CATCGCCGCAGACAAACAT3'	60	278
SIRT1	F:5'GGAACCTTTGCCTCATCTACAT3' R:5'ATTCCTTTTGTGGCGTGG3'	60	164
IL-10	F:5'TGAAGACCCTCAGGATGCG3' R:5'TCCAAGGAGTTGTTCCGTTAG3'	60	291
Catalase	F:5' ACGCTGAGAAGCCTAAGAACG3' R:5' CTAAGCCCTAACCTTTCATTC3'	60	286
SOD2	F:5' CCAGACCTGCCTTACGACTATG3' R:5' CCTTAGGGCTCAGGTTTGCC3'	60	241
Human Serpina4	F:5' GCATCTTCCCAAGTTCTCCATT 3' R:5' ATGCCGGATAAGTCAGCCCA 3'	60	105

eNOS indicates endothelial nitric oxide synthase; IL-10, interleukin 10; qPCR, quantitative polymerase chain reaction; SIRT1, sirtuin 1; SOD2, superoxide dismutase 2.

Measurement of NADPH Oxidase Activity

The enzymatic activity of NADPH oxidase in cell homogenates was assessed by lucigenin-ECL as previously described.¹¹ Fluorescence intensity was continuously monitored for 15 minutes with a fluorescence reader. The chemiluminescent signals observed in the absence of the homogenate were subtracted from the chemiluminescent signals in the samples. The chemiluminescence signal was corrected by the protein concentration of each cell homogenate.

Intracellular ROS Detection

The levels of intracellular reactive oxygen species (ROS) were determined by the ROS-reactive fluorescent indicator 2',7'-dichlorofluorescein diacetate (Molecular Probes, Eugene, OR). Briefly, human umbilical vein endothelial cells were plated overnight at a density of 5×10^5 cells/well in a 12-well plate. After 24 hours of exposure, the medium was removed, and the cells were washed with PBS and then incubated with 10 μ mol/L 2',7'-dichlorofluorescein diacetate for 30 minutes at 37°C. Mean fluorescence intensity of dichlorofluorescein was measured using the BioTek Synergy H1 Hybrid microplate reader (excitation, 485 nm; emission, 530 nm; Biotek Instruments, Inc, Winooski, VT).

Western Blot Analysis

Cell lysates containing 25 μ g of total protein were resolved by SDS-PAGE and transferred to polyvinylidene fluoride membrane (Millipore, Bedford, MA). After being blocked in a buffer containing 5% nonfat milk, the membranes were probed with primary antibodies against SIRT1 (Santa Cruz Biotechnology, Dallas, TX), eNOS (BD Transduction Laboratories, Franklin Lakes, NJ), and β -actin overnight at 4°C. Chemiluminescence was detected using an ECL-Plus kit (Perkin-Elmer, Foster City, CA).

Statistical Analysis

All analyses were performed with SPSS 17.0 software (SPSS, Chicago, IL). For normally distributed parameters, data are presented as the mean \pm standard deviation. For comparisons of means among patient groups and controls, a standard 1-way ANOVA was used. Categorical variables were compared using the χ^2 test. Because plasma kallistatin levels were not normally distributed according to the Kolmogorov-Smirnov test, the data are presented as the median (minimum-maximum), and the nonparametric Mann-Whitney U test and Kruskal-Wallis test were used for the quantitative variables. Nonparametric bivariate correlations (Spearman coefficients) were used to study the correlations

among the level of plasma kallistatin, the Gensini score, and the level of MDA. Further, linear regression was performed to determine if the medication history affects the kallistatin level. To determine if the plasma kallistatin is the independent risk factor of coronary stenosis, logistic regression was performed. The Mann-Whitney U test was used to compare kallistatin levels in groups according to the number of diseased vessels. In the animal model, data are presented as the mean±standard deviation. Multiple comparisons were made by 1-way ANOVA followed by

Bonferroni post hoc tests. $P<0.05$ indicated statistical significance.

Results

Baseline Characteristics of Patients and Plasma Levels of Kallistatin and MDA

Based on the presence of significant luminal stenosis on coronary angiography, patients were stratified as having

Table 2. Clinical and Biochemical Characteristics of Participants

	No CAD Control (n=132)	CAD (n=321)			P Value
		1-Vessel Disease (n=136)	2-Vessel Disease (n=122)	3-Vessel Disease (n=63)	
Sex, M/F, n	60/72	77/59	80/42	45/18	0.300
Age, y	61±13	65±11	68±12	68±12	<0.001
Kallistatin (µg/mL)	30.0 (15.3-78.9)	21.7 (2.1-55.7)	20.6 (0.8-32.0)	17.0 (0.5-25.1)	<0.001
MDA (nmol/mL)	4.5±1.1	5.7±1.9	5.8±1.4	6.1±2.6	<0.001
Gensini score	5.7±1.3	14.6±3.3	35.9±7.0	57.5±3.6	<0.001
Hypertension, n	73	96	91	48	0.004
Type 2 diabetes mellitus, n	21	25	31	19	0.070
Smoking, n	21	24	26	19	0.076
eGFR, mL/min	97.5±27.1	88.1±20.2	90.9±16.1	91.2±18.4	0.127
TG, mmol/L	1.2±1.1	1.6±1.2	1.5±1.1	1.8±1.2	0.016
TC, mmol/L	3.1±2.1	3.9±1.6	4.1±1.7	3.8±1.5	<0.001
HDL, mmol/L	0.9±0.6	1.1±0.4	1.1±0.4	1.0±0.4	0.001
LDL, mmol/L	1.9±1.6	2.3±1.1	2.5±1.2	2.3±1.0	0.007
RBC, ×10 ¹² /L	4.4±0.5	4.5±0.5	4.3±0.7	4.2±1.0	0.019
WBC, ×10 ⁹ /L	6.1±1.7	6.3±2.2	6.7±2.4	7.2±2.3	0.016
N, ×10 ⁹ /L	7.2±3.1	4.3±2.2	5.8±1.0	5.1±2.3	0.653
N%	63.1±10.7	66.2±11.5	66.2±13.1	65.7±20.0	0.313
TnI, ng/mL	0	0.6±0.3	1.4±0.7	1.3±0.5	0.239
BNP, pg/mL	196.7±58.8	280.8±82.8	315.4±68.3	311.8±96.8	0.593
Albumin, g/L	32.3±18.7	37.6±12.2	38.9±8.5	37.7±9.6	0.001
Aspirin, n	99	113	100	55	0.081
Clopidogrel, n	26	59	75	46	<0.001
β-blocker, n	77	76	86	40	0.070
ACEI/ARB, n	39	65	69	41	<0.001
Statin, n	96	122	106	56	0.001
LMWH, n	11	31	54	35	<0.001
OAC, n	8	12	9	2	0.524
CCB, n	40	49	38	18	0.715
Diuretics, n	39	33	50	22	0.027
Nitrate, n	27	38	45	22	0.021

Data are number (%) and mean (SD). ACEI/ARB indicates angiotensin-converting enzyme inhibitors/angiotensin receptor blocker; BNP, B-type natriuretic peptide; CAD, coronary artery disease; CCB, calcium channel blockers; eGFR, estimated glomerular filtration rate; HDL, high-density lipoprotein; LDL, low-density lipoprotein; LMWH, low-molecular-weight heparins; MDA, malondialdehyde; N, neutrophils; OAC, oral anticoagulant; RBC, red blood cells; TC, total cholesterol; TG, triglyceride; TnI, troponin I; WBC, white blood cell.

1-vessel CAD (n=136), 2-vessel CAD (n=122), or 3-vessel CAD (n=63). Patients without CAD served as controls (n=132). Table 2 shows the clinical characteristics of the 3 CAD groups and the control group. There were no significant differences among the groups in terms of sex ratio, smoking, Troponin I, B-type natriuretic peptide, or estimated glomerular filtration rate. Additionally, there were no significant intergroup differences in the prevalence of diabetes mellitus according to the χ^2 test. The results showed that medication history has no influence on kallistatin level (Table 2).

The differences in the plasma kallistatin values among the 3 patient groups and the CAD-free control groups were significant ($P<0.001$, Kruskal-Wallis test, Table 2). Further statistical analysis using the Mann-Whitney U test to compare groups revealed that the median plasma kallistatin levels in 1-vessel (21.7 mg/L), 2-vessel (20.6 mg/L), and 3-vessel (17.0 mg/L) CAD patients were dramatically lower than those in control patients (30.0 mg/L, $P<0.001$ versus 1-vessel, 2-vessel, and 3-vessel CAD patients) (Figure 1A). Plasma kallistatin levels were significantly different among patients with different severities of CAD ($P=0.006$, 1-vessel versus 2-vessel; $P<0.001$, 1-vessel versus 3-vessel; $P=0.015$ 2-vessel versus 3-vessel). According to Spearman correlation coefficients, there were negative correlations between kallistatin levels and the severity of CAD ($r=-0.346$, $P<0.001$) and MDA levels ($r=-0.572$, $P<0.001$) (Figure 1B and 1C). The results showed that after adjustment to the confounding factor, low plasma level of kallistatin was an independent risk factor of coronary stenosis (Table 3).

Kallistatin Gene Transfer Inhibits Low-Shear Stress–Induced Carotid Artery Plaque Formation in Mice

The apoE^{-/-} mice (n=40) underwent baseline MRI and were randomly assigned to receive control Ad.Null, Ad.HKS, Ad.HKS+L-NAME, or Ad.HKS+NAM for a period of 2 weeks. All mice underwent an MRI scan before they were euthanized. Ad.HKS tail vein injection prevented left carotid plaque formation, as indicated by a dramatic increase in the relative vascular lumen diameter compared with the left carotid artery diameter of Ad.Null-injected apoE^{-/-} mice (Figure 2A through 2C). Similarly, a significant reduction in left carotid artery plaque volume was achieved with Ad.HKS treatment. The protective effect of kallistatin gene delivery was blocked by the NOS inhibitor L-NAME and the SIRT1 inhibitor NAM.

We measured human kallistatin expression in apoE^{-/-} mice by ELISA on day 14 after tail vein injection. Human kallistatin was detected in the plasma of Ad.HKS-treated mice (4.03 ± 2.4 ng/mL, n=8) but not in mice injected with the control virus. We also used real-time PCR to determine

human kallistatin expression in carotid artery. In the Ad.HKS injection group, there was detectable HKS gene expression in carotid artery plaque (human kallistatin mRNA levels 0.02 ± 0.01 [%control]). L-NAME and NAM did not affect the expression of kallistatin, but kallistatin was not detectable in Ad.Null mice. There was no difference in lipid levels (triglycerides, total cholesterol, high-density lipoprotein cholesterol, and low-density lipoprotein cholesterol) between Ad.Null and Ad.HKS apoE^{-/-} mice. MDA and TNF- α levels were significantly increased in Ad.Null apoE^{-/-} mice but were reduced in Ad.HKS-injected apoE^{-/-} mice. Kallistatin's effect was blocked by L-NAME and NAM (Figure 2D and 2E).

Immunohistochemistry verified that vascular endogenous kallistatin expression was most apparent in adventitial layers of the arterial wall in the normal C57BL/6 mice. Weak immunostaining for kallistatin was detected throughout the intima and media. In apoE^{-/-} mice, a strong positive kallistatin staining was observed in the adventitia of the control right carotid artery. Compared with the contralateral segments of the right carotid artery, kallistatin expression was not increased in the neointimal lesions in the left carotid artery (n=6) (Figure 2F). These results showed that the endogenous mouse kallistatin expression was decreased in atherosclerotic plaques compared with the contralateral artery of apoE^{-/-} mice and normal vascular tissue.

Kallistatin Reduces Low-Shear Stress–Induced Inflammatory Cell Accumulation and Oxidative Stress and Increases eNOS and SIRT1 Expression in Mice

Hematoxylin and eosin staining showed well-developed atherosclerotic plaques in the left carotid arteries of Ad.Null apoE^{-/-} mice (Figure 3A). Ad.HKS injection significantly reduced the plaque area, but this effect was blocked by L-NAME and NAM treatment (Figure 3A). As shown in oil red O staining (Figure 3B), the areas in Ad.HKS apoE^{-/-} mice that stained positive for lipid in the lesion of carotid artery were smaller than those in Ad.Null apoE^{-/-} mice. Monocyte/macrophage accumulation in the plaque was determined by immunohistochemical staining against CD68 (Figure 3D), a specific marker for monocytes and macrophages. We found that kallistatin gene transfer significantly reduced monocyte/macrophage accumulation in the carotid artery compared with Ad.Null injection (29 ± 4 versus 17.1 ± 2.6 per high-power field, n=5, $P<0.01$, Figure 3D through 3F). We also found that kallistatin gene transfer significantly decreased superoxide formation (n=5, Figure 3C through 3G), as determined by the fluorescent probe dihydroethidium in the carotid artery. Morphometric analysis revealed total wall fluorescence to be significantly

decreased in Ad.HKS mice compared with Ad.Null mice. However, the beneficial effects of kallistatin were blocked by L-NAME and NAM treatment. When we used immunohistochemical analysis to investigate the expression of TNF- α in the plaque area, we found that kallistatin gene transfer significantly decreased TNF- α expression (n=5, Figure 3E) compared with that in mice injected with Ad.Null. Double

staining for eNOS/CD31 and SIRT1/CD31 showed that Ad.HKS increased eNOS and SIRT1 expression and that the majority of eNOS-positive and SIRT1-positive cells were also CD31 positive. Our quantitative analysis showed that L-NAME inhibited eNOS expression but did not entirely block SIRT1 expression, whereas NAM completely inhibited SIRT1 and eNOS expression (Figure 3G and 3H).

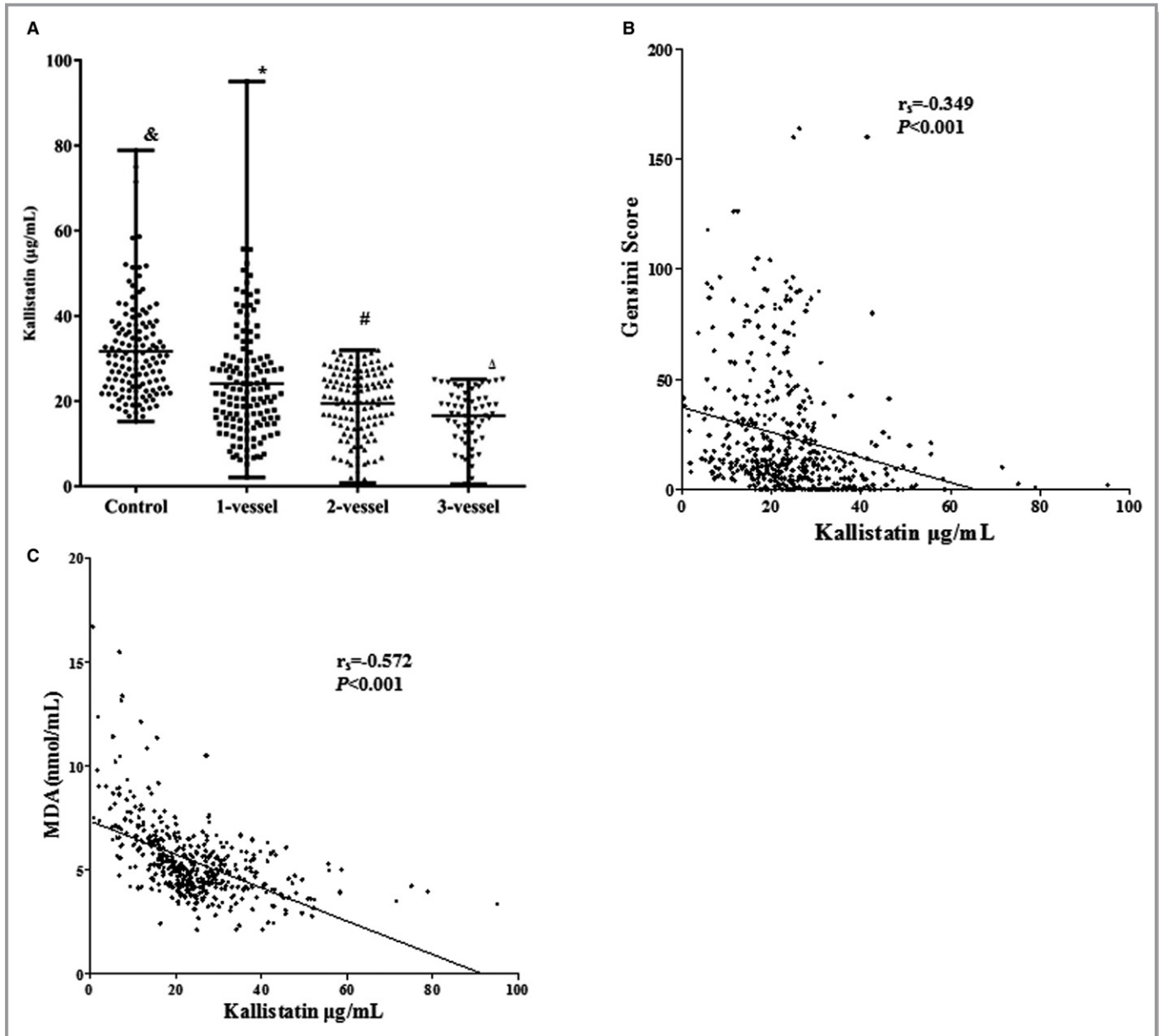


Figure 1. Kallistatin levels in the study groups. **A**, Dispersion graph of plasma kallistatin levels in patients classified according to the number of diseased vessels. There was a statistically significant difference among patients categorized by the number of diseased vessels ($\&P < 0.001$, Control vs 1-vessel, 2-vessel, or 3-vessel disease; $*P = 0.006$, 1-vessel disease vs 2-vessel disease; $\Delta P < 0.001$, 1-vessel disease vs 3-vessel disease; $\#P = 0.015$, 2-vessel disease vs 3-vessel disease). **B**, A strong negative correlation between plasma kallistatin levels and Gensini score was observed in all patients (n=456, $r = -0.346$, $P < 0.001$). **C**, There was a strong negative correlation between plasma kallistatin levels and MDA levels in all patients (n=456, $r = -0.572$, $P < 0.001$). MDA indicates malondialdehyde.

Kallistatin Increases eNOS, SIRT1, IL-10, SOD2, and Catalase Expression in Mice

We determined the potential involvement of antioxidative stress mediator expression in low-shear stress-induced carotid artery injury in mice. eNOS, SIRT1, interleukin (IL)-10, superoxide dismutase (SOD)2, and catalase gene expression in carotid artery plaque were significantly upregulated by kallistatin treatment, and the effect was blocked by pretreatment with NAM. However, L-NAME abolished kallistatin-induced eNOS, IL-10, superoxide dismutase 2 (SOD2), and catalase gene expression but did not block SIRT1 synthesis (Figure 4A through 4E).

Kallistatin Inhibits TNF- α -Mediated Oxidative Stress via the SIRT1-eNOS Signaling Pathway in Human Endothelial Cells

TNF- α treatment significantly increased intracellular NADPH oxidase activity, while kallistatin significantly blocked these effects in human endothelial cells. These effects were eliminated by the NOS inhibitor L-NAME and the SIRT1 inhibitor NAM.

We were able to determine whether or not kallistatin inhibited TNF α -induced intracellular ROS accumulation using an ROS-sensitive fluorescence indicator, 2',7'-dichlorofluorescein diacetate. The accumulation of ROS was elevated by 2-fold after a 24-hour exposure to TNF α . Preincubation with kallistatin abrogated TNF α -induced ROS accumulation (Figure 5B). These effects were blocked by the NOS inhibitor L-NAME and the SIRT1 inhibitor NAM.

Moreover, kallistatin treatment in human umbilical vein endothelial cells induced a noticeable increase in SIRT1 and eNOS expression, as evidenced by qPCR and Western blot analyses (Figure 5B through 5D). However, the stimulatory effects of kallistatin on SIRT1 and eNOS were blocked by SIRT1 and/or nitric oxide synthase inhibition. L-NAME did not

block kallistatin-induced SIRT1 expression, indicating that SIRT1 is upstream of eNOS.

Discussion

In the present study we demonstrated for the first time that plasma kallistatin levels are decreased in CAD patients and are inversely associated with the severity of CAD. In addition, we showed negative correlations between kallistatin levels and the oxidative stress marker, MDA, in patients. Moreover, kallistatin gene delivery prevented low-shear stress-induced carotid plaque formation in apoE^{-/-} mice and inhibited vascular oxidative stress and carotid plaque formation through the SIRT1/eNOS pathway. An *in vitro* study with cultured endothelial cells further confirmed that kallistatin inhibited TNF- α -induced oxidative stress formation through the SIRT1-eNOS pathway. These findings indicate that kallistatin is a potential therapeutic target for the treatment of atherosclerosis.

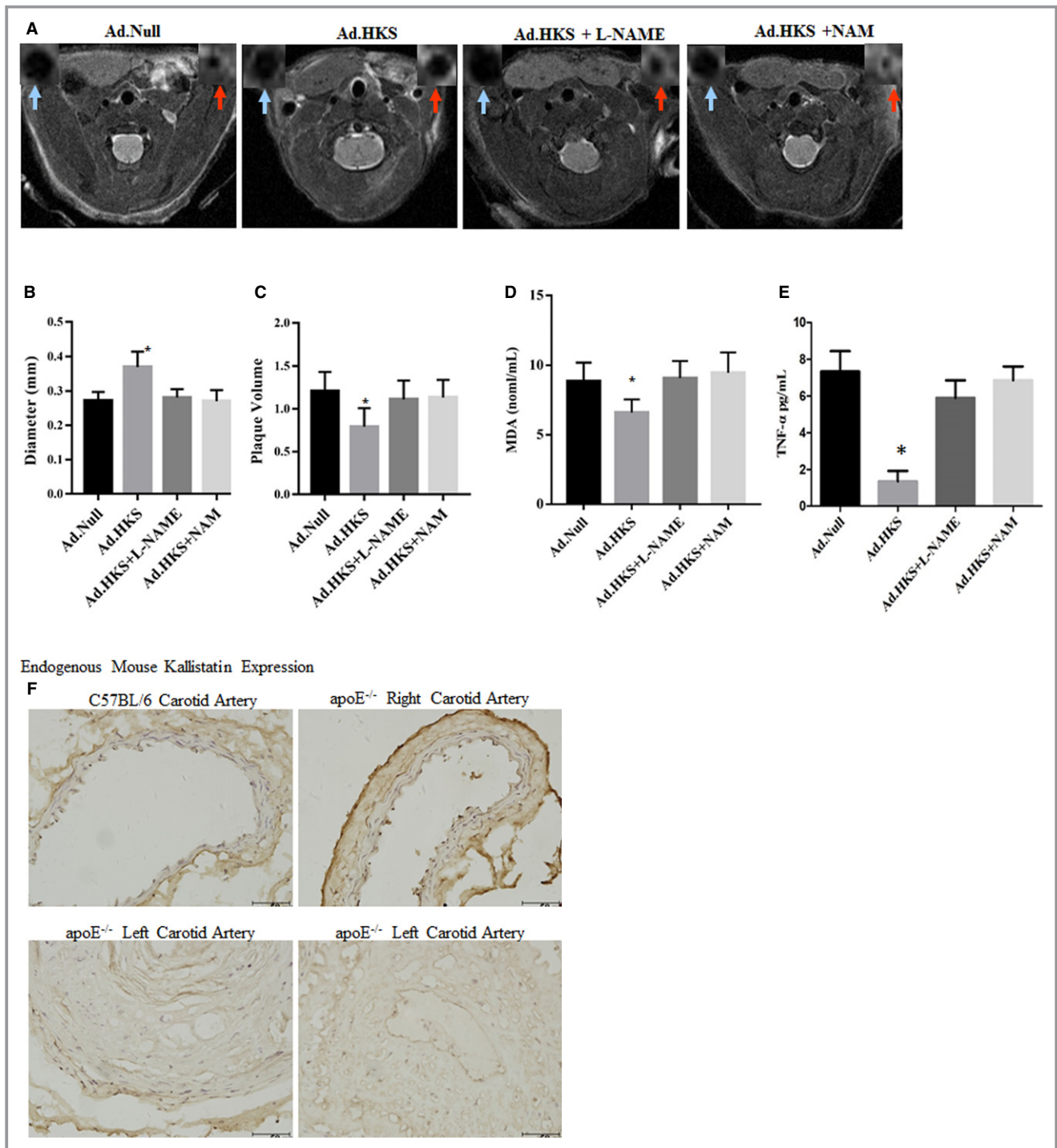
Kallistatin is an endogenous plasma protein that has pleiotropic functions.⁸ Kallistatin was first identified as a tissue kallikrein-binding protein that specifically inhibits tissue kallikrein activity.¹⁸ Kallistatin via its heparin-binding site competes with the binding of VEGF, TNF- α , HMGB1, and TGF- β to their respective receptors by interacting with cell-surface heparin sulfate proteoglycans, leading to antiangiogenic, anti-inflammatory, and antifibrotic activity.^{9,10,17,19} In human studies circulating kallistatin levels were shown to be decreased in patients with liver disease, sepsis, severe pneumonia, and pulmonary tuberculosis.²⁰⁻²³ The decrease in kallistatin levels reflects the extent of cirrhosis and the severity and outcome of sepsis.²⁰⁻²² Moreover, plasma kallistatin levels are inversely associated with adiposity, adverse lipid profiles, and inflammation in apparently healthy black adolescents.²⁴ Based on previous studies, kallistatin plays a role in the regulation of vascular homeostasis. Atherosclerosis is the principal cause of coronary artery disease, but little is known about the effects of kallistatin on the risk of atherosclerosis. In this study we measured the kallistatin levels in 321 CAD patients and 132 non-CAD controls whose status were all confirmed by angiography. Our results showed that kallistatin levels were significantly decreased in CAD patients and revealed negative correlations between kallistatin levels and the severity of CAD and the oxidative stress marker MDA. Elevated kallistatin levels have been reported in patients with type 2 diabetes mellitus with diabetic vascular complications.²⁵ Angiogenesis is a critical pathological characteristic of diabetic vascular complications. Thus, as an antiangiogenic protein, kallistatin may be reactively increased in patients with diabetic vascular complications. In this study we did not exclude patients with

Table 3. Logistic Regression Analysis of Variables

Variable	P Value	OR	95% CI
Kallistatin, $\mu\text{g/mL}$	<0.001	0.890*	0.861 to 0.920
DM (yes or no)	0.787	0.912	0.466 to 1.783
Age, y	0.798	1.004	0.977 to 1.031
Hypertension (yes or no)	0.103	0.612	0.339 to 1.105
Albumin, g/L	0.032	0.926	0.863 to 0.994
WBC ($\times 10^9/\text{L}$)	0.119	1.122	0.971 to 1.298

CI indicates confidence interval; DM, diabetes mellitus; OR, odds ratio; WBC, white blood cell.

*Every 1 $\mu\text{g/mL}$ decline in the kallistatin level was associated with an 11% increased risk of coronary stenosis.



Endogenous Mouse Kallistatin Expression

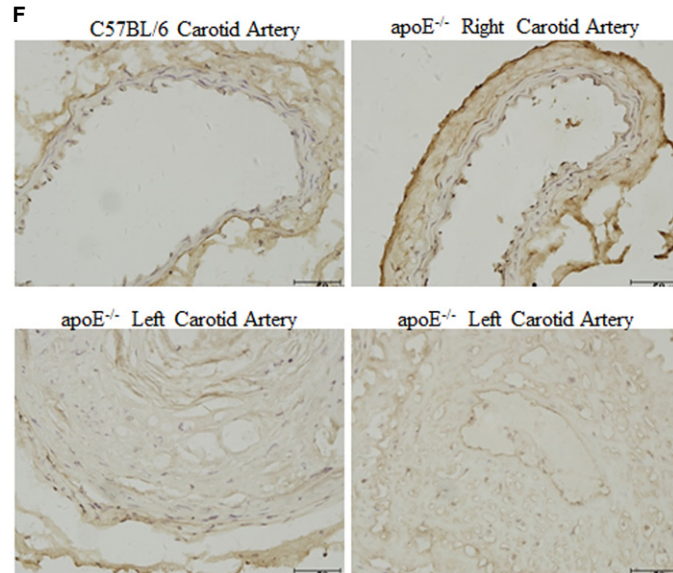


Figure 2. Kallistatin inhibited low-shear stress–induced carotid artery plaque formation. **A**, Representative magnetic resonance images in cross-sectional views through the carotid arteries. The red arrow indicates the cross section of the left carotid artery, and the blue arrow indicates the cross section of the right carotid artery. **B**, Quantitative analysis of left carotid artery diameter in the Ad.HKS and Ad.Null groups. L-NAME and NAM blocked the effects of kallistatin ($n=10$, $*P<0.05$ vs the Ad.Null-, L-NAME-, or NAM-treated groups). **C**, Quantitative analysis of left carotid artery plaque volume in the Ad.HKS and Ad.Null groups. L-NAME and NAM blocked the effect of kallistatin; $n=10$ ($*P<0.05$ vs the Ad.Null-, L-NAME- or NAM-treated groups). **D**, Plasma MDA levels in apoE^{-/-} mice. **E**, Plasma TNF- α levels in apoE^{-/-} mice. **F**, Distribution of mouse kallistatin expression in atherosclerotic lesions and normal vascular tissue. Data are presented as the mean \pm SEM; $n=10$, $*P<0.05$ vs the Ad.Null-, L-NAME-, or NAM-treated groups. Ad.HKS indicates adenovirus containing kallistatin cDNA; Ad.Null, adenovirus containing null cDNA; L-NAME, N^o-nitro-L-arginine methyl ester; MDA, malondialdehyde; NAM, nicotinamide; SEM, standard error of the mean; TNF- α , tumor necrosis factor- α .

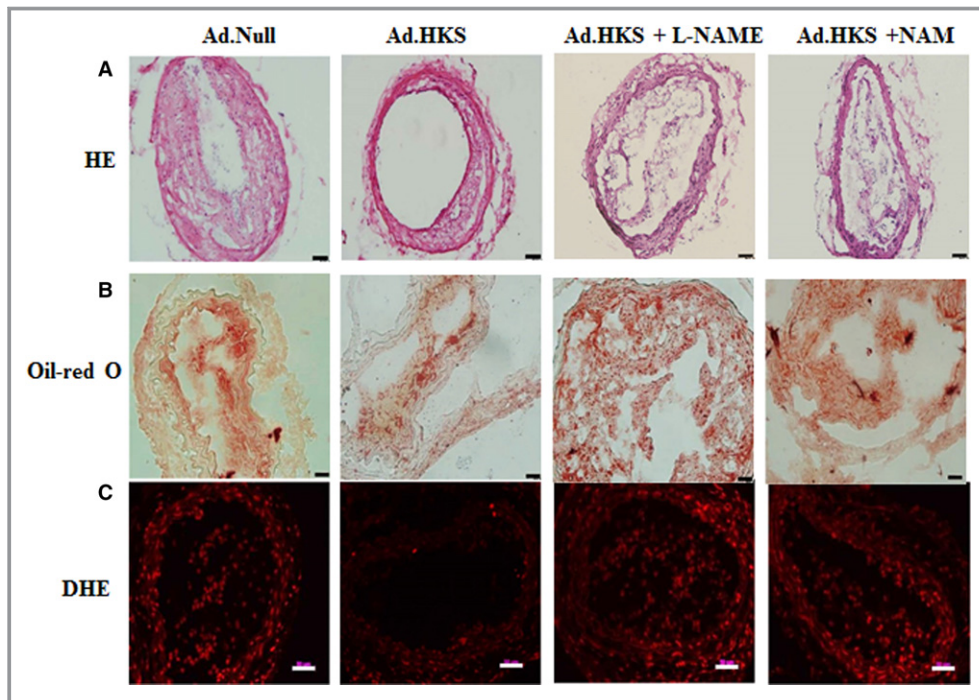


Figure 3. Kallistatin led to morphological changes in the atherosclerotic plaques of apoE^{-/-} mice. **A**, Representative images of HE staining. Original magnification is $\times 10$ ($n=5$ in each group). **B**, Oil red O staining of carotid specimens of mice in the Ad.Null group, the Ad.HKS group, and L-NAME- or NAM-treated groups ($n=5$ in each group). **C**, Representative images of superoxide formation labeled by the red fluorescence dye dihydroethidium in the carotid artery of Ad.Null mice, Ad.HKS mice, Ad.HKS+L-NAME mice, and Ad.HKS+NAM mice ($n=5$ in each group). **D**, Representative images of CD68 immunostaining in lesion areas of the left carotid artery ($n=5$ in each group). **E**, Immunohistochemical assessments of the protein level of TNF- α in carotid plaque ($n=5$ in each group). **F**, Quantitative analyses of CD68-positive cells in the 4 groups ($n=5$ in each group, $*P<0.05$ vs the Ad.Null-, L-NAME-, or NAM-treated groups). **G**, Fluorescence intensity was measured by a fluorescence microscope and quantified with Image software ($n=5$ in each group, $*P<0.05$ vs the Ad.Null-, L-NAME-, or NAM-treated groups). **H**, Colocalization of PE red fluorescence (SIRT1) and FITC green fluorescence (CD31) within plaques ($\times 40$ magnification) in the carotid arteries of the Ad.Null, Ad.HKS, Ad.HKS+L-NAME, and Ad.HKS+NAM groups with labeled cell nuclei (blue) ($n=5$ in each group). Regions shown at a higher magnification (far right) are indicated by yellow boxes. Endothelial cell-specific SIRT1 fluorescence was measured on the luminal side of the internal elastic lamina only and expressed in mean pixel intensity per area ($n=5$ in each group, $^{\#}P<0.05$ vs the Ad.Null- and NAM-treated groups). **I**, Colocalization of PE red fluorescence (eNOS) and FITC green fluorescence (CD31) within carotid artery plaques ($\times 40$ magnification) of the 4 groups with labeled cell nuclei (blue). Regions shown at a higher magnification (far right) are indicated by yellow boxes. Endothelial cell-specific eNOS fluorescence was measured on the luminal side of the internal elastic lamina only and expressed in mean pixel intensity per area ($*P<0.05$ vs the Ad.Null-, L-NAME-, or NAM-treated groups). We observed that red fluorescence (SIRT1, eNOS) and green fluorescence (CD31) signals were colocalized in the Ad.HKS group. Scale bar=50 μm . Ad.HKS indicates adenovirus containing kallistatin cDNA; Ad.Null, adenovirus containing null cDNA; DAPI, 4',6-diamidino-2-phenylindole; DHE, dihydroethidium; eNOS, endothelial nitric oxide synthase; FITC, fluorescein isothiocyanate; HE, hematoxylin and eosin; L-NAME, N^o-nitro-L-arginine methyl ester; NAM, nicotinamide; PE, phycoerythrin; SIRT1, sirtuin 1; TNF- α , tumor necrosis factor- α .

diabetes mellitus, and there was no significant intergroup difference in the prevalence of diabetes mellitus.

The causes of decreased plasma kallistatin in CAD patients are not yet known. Oxidative stress exhibits opposite effects on kallistatin expression by down- or up-regulation depending

on oxygen concentration.²⁶ High oxygen inhibits kallistatin expression, whereas mild oxygen stimulates kallistatin synthesis in human endothelial cells and mouse kidney. Our previous report showed that kallistatin expression is down-regulated by oxidative stress via activating Jun amino-terminal

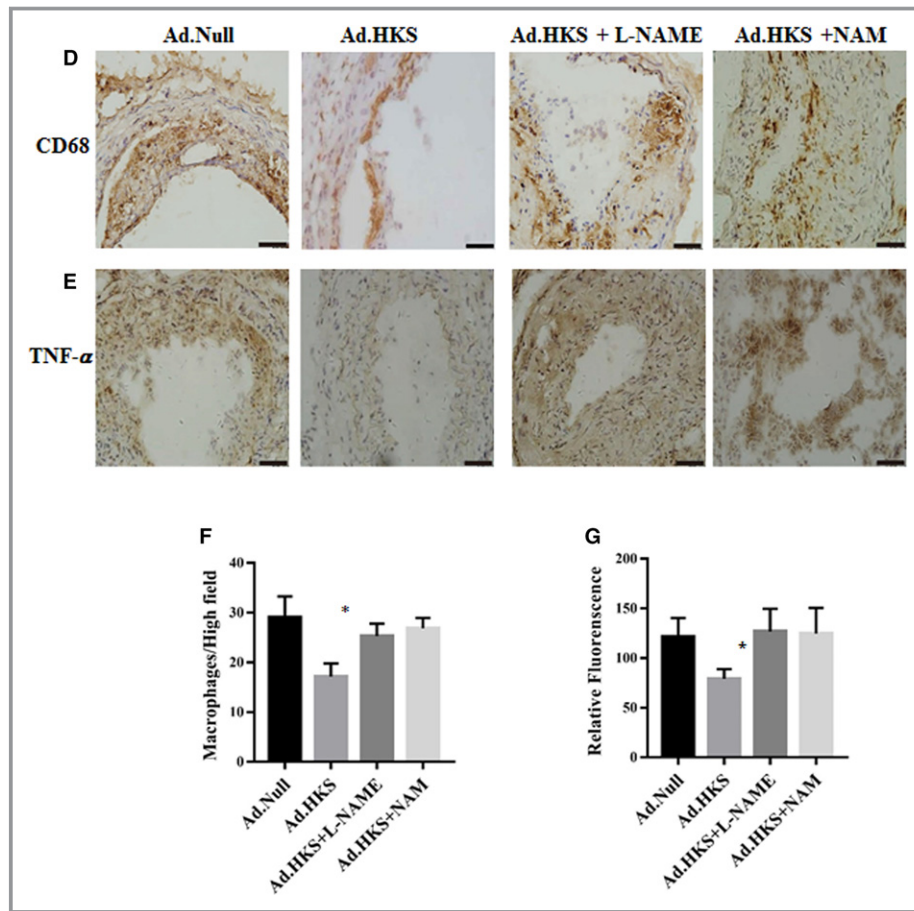


Figure 3. Continued

kinases–FOXO1 pathway in endothelial cells.²⁷ Kallistatin is mainly expressed in the liver and is widely distributed in the cardiovascular system, blood vessels, and endothelial cells.²⁸ Immunohistochemistry shows that endogenous mouse kallistatin expression was not increased in atherosclerotic plaques compared with contralateral artery of apoE^{-/-} mice and normal vascular tissue. Our study suggests that decreased plasma kallistatin levels may be the result of overconsumption of kallistatin in patients under oxidative stress conditions and suppressed kallistatin synthesis conditions in endothelial cells.²⁷ The involvement of kallistatin in coronary syndrome and at different stages of diabetes mellitus is complicated, and it remains to be further investigated in future studies.

Inflammation is triggered by oxidative stress, and inflammation is 1 of the manifestations of oxidative stress. The mechanism by which inflammation induces oxidative stress, or how oxidative stress triggers inflammation, is unclear.²⁹ As a plasma protein, kallistatin is expressed in vascular tissues,³⁰ and it exerts anti-inflammatory and antioxidative stress functions.⁹ Oxidative stress suppresses kallistatin expression in cultured endothelial cells.²⁷ We further investigated the effects of kallistatin on low-shear stress–induced carotid

artery atherosclerosis in a mouse model. Serum oxidative stress markers have been reported to be significantly increased in apoE^{-/-} mice,³¹ and low-shear stress–induced damage can lead to local plaque formation and endothelial dysfunction.³² We used Ad.HKS virus tail vein injection to increase human kallistatin protein levels in a partial carotid artery ligation apoE^{-/-} mouse model. Mice that received the Ad.Null virus exhibited significant carotid artery plaque formation, inflammation, and oxidative stress. The diameter of the left artery was also very small compared with that of the right artery. Kallistatin gene delivery significantly increased the left carotid diameter and decreased carotid plaque formation. In the group that received the human kallistatin gene, macrophage accumulation, oxidative stress, TNF- α , and MDA levels were significantly decreased, and SIRT1 and eNOS expression were increased. CD31 has a key role in the maintenance of vascular integrity: immunofluorescence staining results showed there is a strong diffuse staining of CD31 in the carotid artery plaque in the Ad.HKS group when compared with the Ad.Null group. Based on our results, the antiatherosclerotic effect of kallistatin is dependent on its anti-inflammatory and antioxidative stress properties. We then

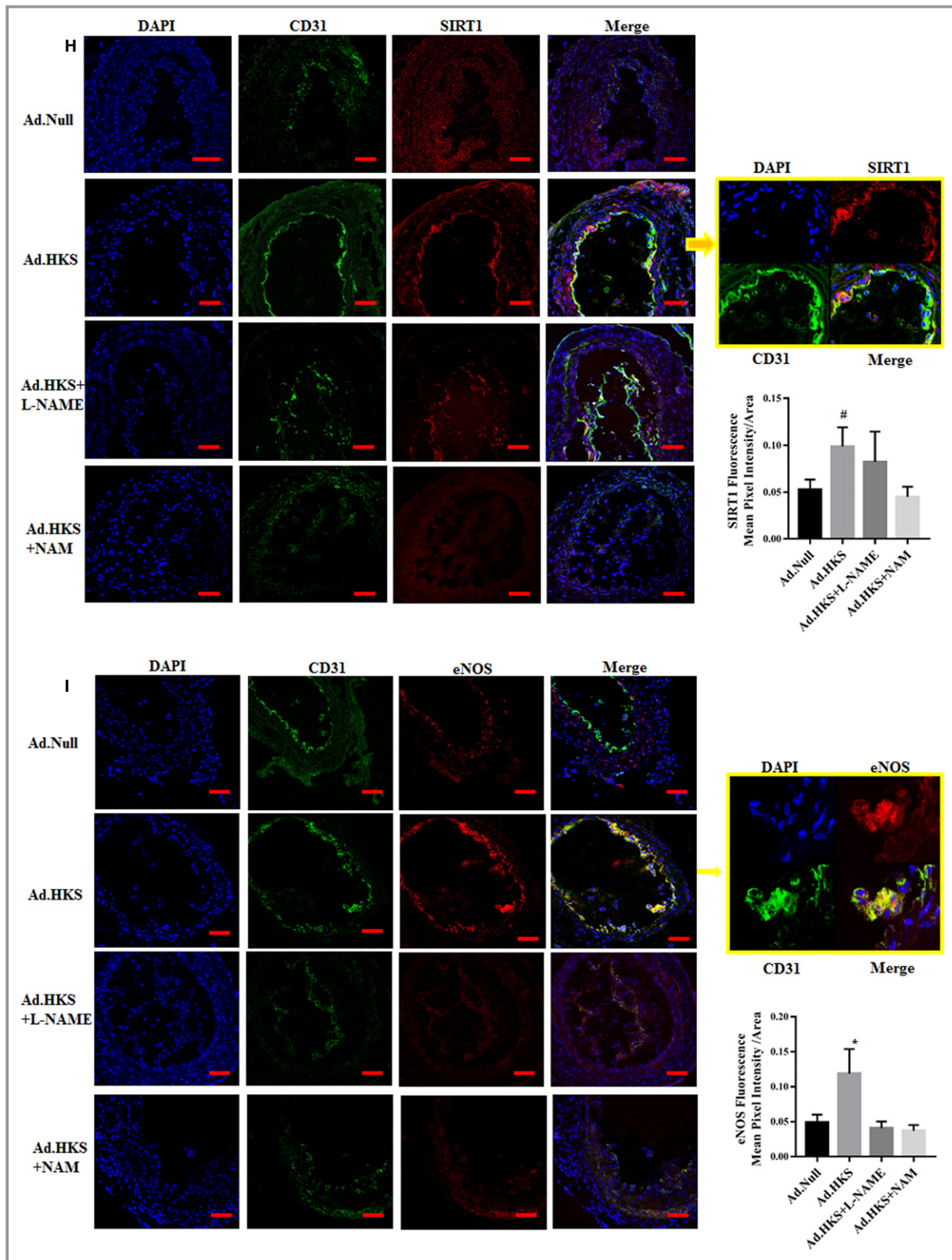


Figure 3. Continued

used the eNOS inhibitor L-NAME and the SIRT1 inhibitor NAM on a murine atherosclerotic model to explore the roles of eNOS and SIRT1 in the known beneficial effect of kallistatin.

Our results clearly showed that L-NAME and NAM could block the protective effect of kallistatin and that the mice in the Ad.HKS+L-NAME and Ad.HKS+NAM groups had significant

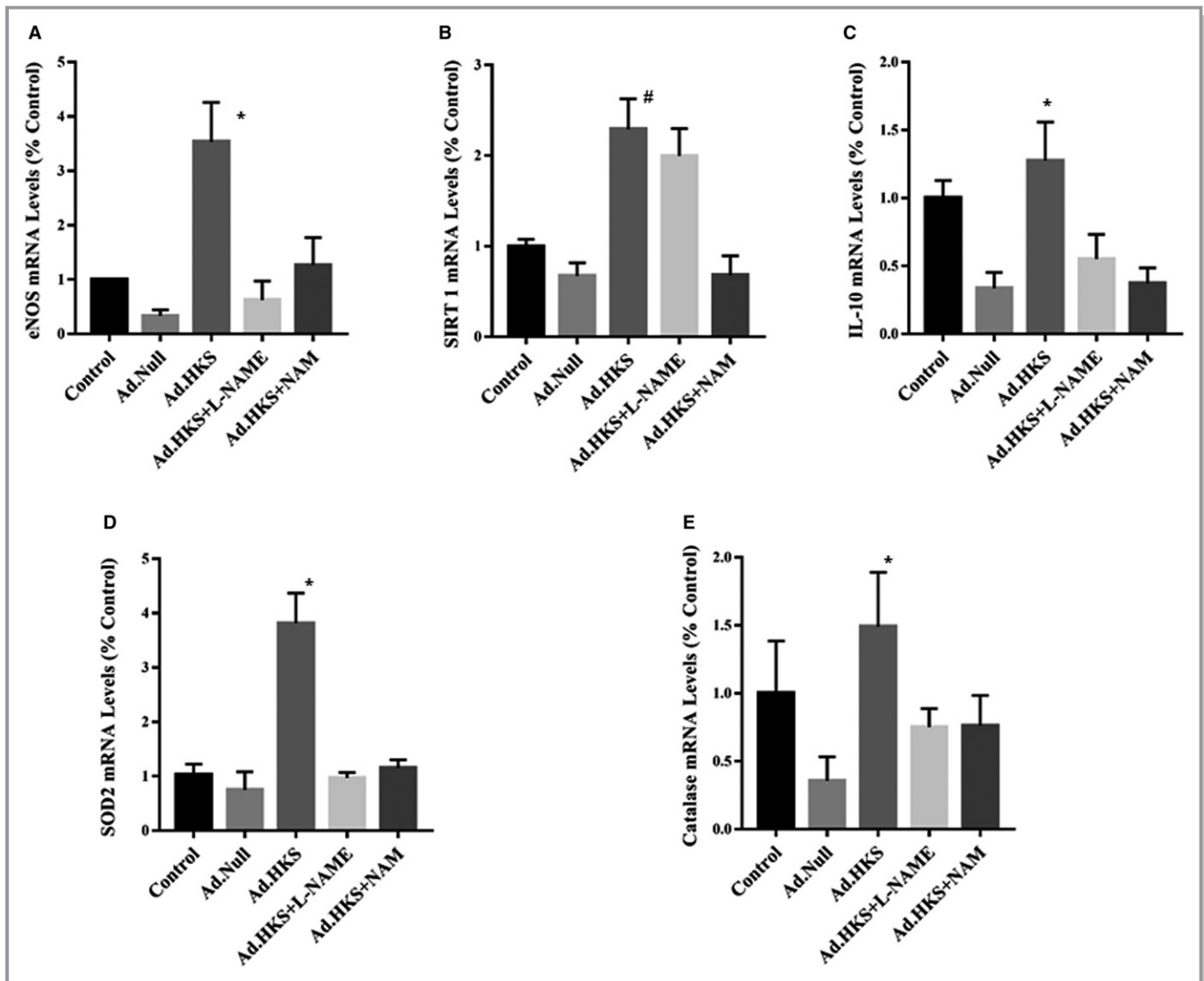


Figure 4. Effect of kallistatin on eNOS (A), SIRT1 (B), IL-10 (C), SOD2 (D), and catalase (E) expression in low-shear stress–induced carotid artery plaques in vivo (n=5 in each group, * $P<0.05$ vs the Ad.Null-, L-NAME-, or NAM-treated groups. # $P<0.05$ vs the Ad.Null- and NAM-treated groups). Ad.HKS indicates adenovirus containing kallistatin cDNA; Ad.Null, adenovirus containing null cDNA; eNOS, endothelial nitric oxide synthase; IL, interleukin; L-NAME, N^o-nitro-L-arginine methyl ester; NAM, nicotinamide; SIRT1, sirtuin 1; SOD2, superoxide dismutase 2.

plaque formation. Partial carotid artery ligation with Ad.Null injection in the apoE^{-/-} model resulted in low eNOS, SIRT1, IL-10, SOD2 and catalase expression, and Ad.HKS significantly increased eNOS, SIRT1, IL-10, SOD2, and catalase expression. NAM completely blocked the effect of kallistatin, whereas L-NAME reduced kallistatin-induced eNOS, IL-10, catalase, and SOD2 expression but did not block SIRT1 expression.

SIRT1 is an NAD⁺-dependent class III histone deacetylase that mediates the effects of caloric restriction on lifespan and metabolic pathways in various organisms.³³ SIRT1 and eNOS play a central role in improving endothelium-dependent vascular function.³⁴ Our recent study showed that kallistatin prevents endothelial progenitor cell senescence by regulating the microRNA-34a–SIRT1 pathway.³⁵ Laminar shear stress

enhances endothelial function by increasing SIRT1 activity and activating eNOS.³⁶ Overexpression of the human SIRT1 gene in endothelial cells of atherosclerotic mice results in increased eNOS expression.³⁷ There is also considerable evidence that SIRT1 can upregulate cellular antioxidant enzymes such as SOD2 and catalase.^{38,39} In this study kallistatin increased the expression of SOD2, a mitochondria-specific isoform of SOD that can attenuate mitochondrial oxidative damage, through the SIRT1–eNOS pathway. Moreover, Kallistatin increased the expression of both SOD2 and catalase, suggesting that mitochondrial antioxidative capacity was increased. Our study consistently showed that oxidative stress is significantly decreased in the plasma and vascular wall after kallistatin treatment. In the in vitro study, kallistatin

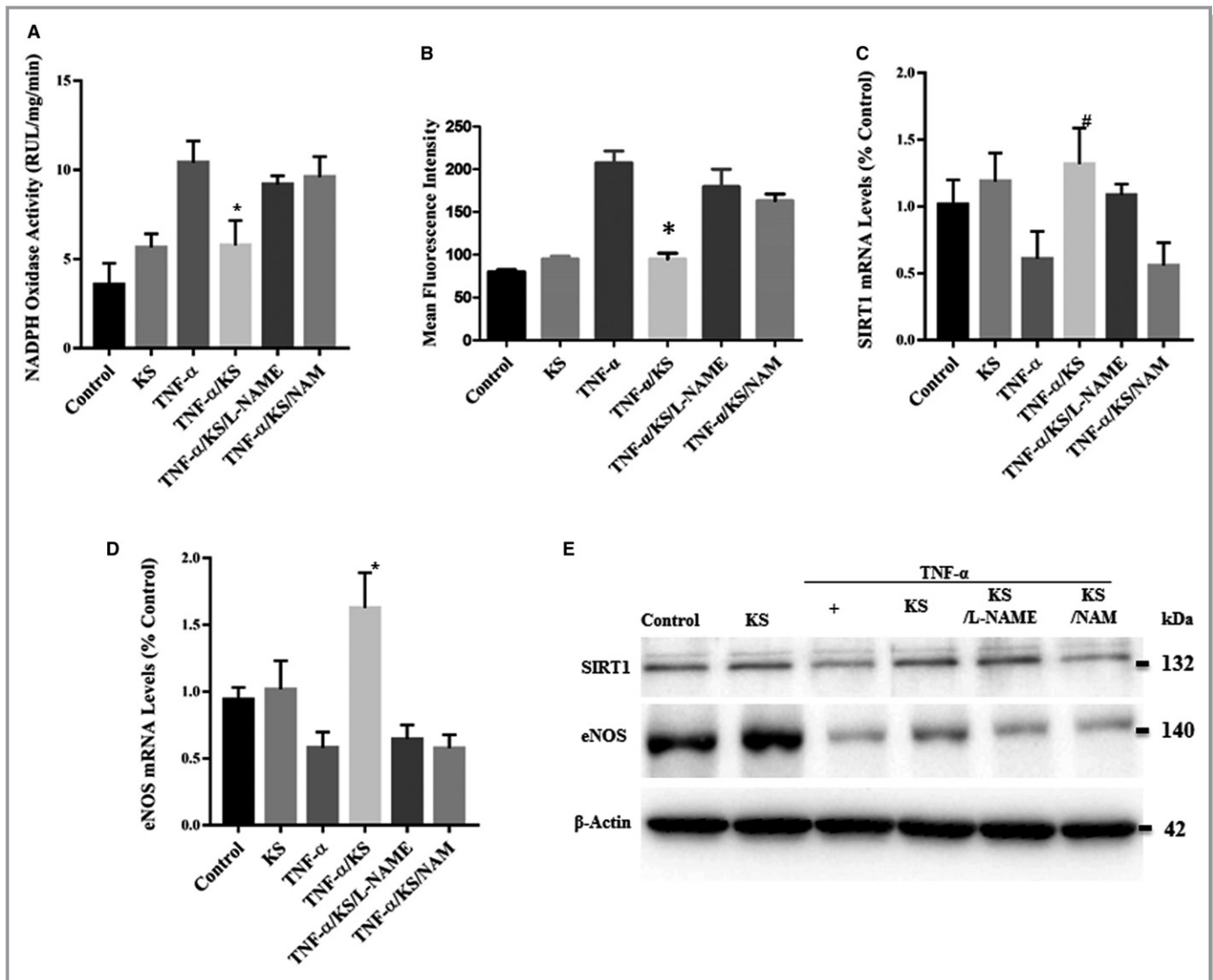


Figure 5. Effect of kallistatin protein (KS) on TNF- α -induced HUVECs. NADPH oxidase activity (A), intracellular ROS accumulation (B), relative SIRT1 mRNA expression levels (C), relative eNOS mRNA expression levels (D), and SIRT1 and eNOS protein expression (E). Data are presented as the mean \pm SEM (n=5, *P<0.05 vs the TNF- α , TNF- α +KS+L-NAME, and TNF- α +KS+L-NAME groups. #P<0.05 vs the TNF- α and TNF- α +KS+L-NAME groups). eNOS indicates endothelial nitric oxide synthase; HUVEC, human umbilical vein endothelial cells; KS, kallistatin; L-NAME, N^ω-nitro-L-arginine methyl ester; NAM, nicotinamide; ROS, reactive oxygen species; SIRT1, sirtuin 1; TNF- α , tumor necrosis factor- α .

inhibited TNF- α -mediated oxidative stress and increased SIRT1 and eNOS expression. NAM administration abolished kallistatin-induced SIRT1 and eNOS expression, whereas L-NAME did not inhibit SIRT1 expression, confirming that SIRT1 is an upstream activator of eNOS.

This study shows that kallistatin is negatively associated with the presence and severity of CAD in patients and that high expression of kallistatin prevents carotid artery plaque formation and oxidative stress accumulation in low-shear stress-induced plaques in mice. Kallistatin may thus serve as a potential therapeutic target for the treatment of CAD.

This study has some limitations, which should be pointed out. The small patient population and the retrospective

case-control study do not allow us to draw a causation hypothesis about low kallistatin level and the occurrence of coronary heart disease. Hospital-based CAD-free controls may cause selection bias.

Sources of Funding

This work was supported by grants from the National Natural Science Foundation of China (81470401, 81770452 to Yao, 81300249 to Jing Lu), Jiangsu Provincial Key Medical Discipline Laboratory ZDXKA2016023, Jiangsu Provincial Key Research and Development Program BE2016785, and the National Institutes of Health grant HL118516 (Chao).

Disclosures

None.

References

- Nichols M, Townsend N, Scarborough P, Rayner M. Cardiovascular disease in Europe 2014: epidemiological update. *Eur Heart J*. 2014;35:2929.
- Roth GA, Huffman MD, Moran AE, Feigin V, Mensah GA, Naghavi M, Murray CJ. Global and regional patterns in cardiovascular mortality from 1990 to 2013. *Circulation*. 2015;132:1667–1678.
- Fishbein MC, Fishbein GA. Arteriosclerosis: facts and fancy. *Cardiovasc Pathol*. 2015;24:335–342.
- Khot UN, Khot MB, Bajzer CT, Sapp SK, Ohman EM, Brener SJ, Ellis SG, Lincoff AM, Topol EJ. Prevalence of conventional risk factors in patients with coronary heart disease. *JAMA*. 2003;290:898–904.
- Gimbrone MA Jr, García-Cardeña G. Endothelial cell dysfunction and the pathobiology of atherosclerosis. *Circ Res*. 2016;118:620–636.
- Huang X, Zhang J, Liu J, Sun L, Zhao H, Lu Y, Wang J, Li J. C-reactive protein promotes adhesion of monocytes to endothelial cells via NADPH oxidase-mediated oxidative stress. *J Cell Biochem*. 2012;113:857–867.
- Goszcz K, Deakin SJ, Duthie GG, Stewart D, Leslie SJ, Megson IL. Antioxidants in cardiovascular therapy: panacea or false hope? *Front Cardiovasc Med*. 2015;2:29.
- Chao J, Bledsoe G, Chao L. Protective role of kallistatin in vascular and organ injury. *Hypertension*. 2016;68:533–541.
- Yin H, Gao L, Shen B, Chao L, Chao J. Kallistatin inhibits vascular inflammation by antagonizing tumor necrosis factor- α -induced nuclear factor κ B activation. *Hypertension*. 2010;56:260–267.
- Miao RQ, Agata J, Chao L, Chao J. Kallistatin is a new inhibitor of angiogenesis and tumor growth. *Blood*. 2002;100:3245–3252.
- Shen B, Hagiwara M, Yao YY, Chao L, Chao J. Salutary effect of kallistatin in salt-induced renal injury, inflammation, and fibrosis via antioxidative stress. *Hypertension*. 2008;51:1358–1365.
- Gao L, Yin H, Smith RS Jr, Chao L, Chao J. Role of kallistatin in prevention of cardiac remodeling after chronic myocardial infarction. *Lab Invest*. 2008;88:1157–1166.
- Yiu WH, Wong DW, Wu HJ, Li RX, Yam I, Chan LY, Leung JC, Lan HY, Lai KN, Tang SC. Kallistatin protects against diabetic nephropathy in db/db mice by suppressing AGE-RAGE-induced oxidative stress. *Kidney Int*. 2016;89:386–398.
- Gensini GG. A more meaningful scoring system for determining the severity of coronary heart disease. *Am J Cardiol*. 1983;51:606.
- Ma JX, Yang Z, Chao J, Chao L. Intramuscular delivery of rat kallikrein-binding protein gene reverses hypotension in transgenic mice expressing human tissue kallikrein. *J Biol Chem*. 1995;270:451–455.
- Yao Y, Jiang Y, Sheng Z, Zhang Y, An Y, Yan F, Ma G, Liu N, Teng G, Cheng Z. Analysis of in situ and ex vivo $\alpha_5\beta_3$ integrin expression during experimental carotid atherogenesis. *Int J Nanomed*. 2012;7:641–649.
- Li P, Guo Y, Bledsoe G, Yang ZR, Fan H, Chao L, Chao J. Kallistatin treatment attenuates lethality and organ injury in mouse models of established sepsis. *Crit Care*. 2015;19:200.
- Chao J, Chao L. Biochemistry, regulation and potential function of kallistatin. *Biol Chem Hoppe Seyler*. 1995;376:705–713.
- Guo Y, Li P, Bledsoe G, Yang ZR, Chao L, Chao J. Kallistatin inhibits TGF- β -induced endothelial-mesenchymal transition by differential regulation of microRNA-21 and eNOS expression. *Exp Cell Res*. 2015;337:103–110.
- Cheng Z, Lv Y, Pang S, Bai R, Wang M, Lin S, Xu T, Spalding D, Habib N, Xu R. Kallistatin, a new and reliable biomarker for the diagnosis of liver cirrhosis. *Acta Pharm Sin B*. 2015;5:194–200.
- Lin WC, Chen CW, Chao L, Chao J, Lin YS. Plasma kallistatin in critically ill patients with severe sepsis and septic shock. *PLoS One*. 2017;12:e0178387.
- Lin WC, Lu SL, Lin CF, Chen CW, Chao L, Chao J, Lin YS. Plasma kallistatin levels in patients with severe community-acquired pneumonia. *Crit Care*. 2013;17:R27.
- De Groote MA, Sterling DG, Hraha T, Russell TM, Green LS, Wall K, Kraemer S, Ostroff R, Janjic N, Ochsner UA. Discovery and validation of a six-marker serum protein signature for the diagnosis of active pulmonary tuberculosis. *J Clin Microbiol*. 2017;55:3057–3071.
- Zhu H, Chao J, Kotak I, Guo D, Parikh SJ, Bhagatwala J, Dong Y, Patel SY, Houk C, Chao L, Dong Y. Plasma kallistatin is associated with adiposity and cardiometabolic risk in apparently healthy African American adolescents. *Metabolism*. 2013;62:642–646.
- McBride JD, Jenkins AJ, Liu X, Zhang B, Lee K, Berry WL, Janknecht R, Griffin CT, Aston CE, Lyons TJ, Tomasek JJ, Ma JX. Elevated circulation levels of an antiangiogenic SERPIN in patients with diabetic microvascular complications impair wound healing through suppression of Wnt signaling. *J Invest Dermatol*. 2014;134:1725–1734.
- Chao J, Guo Y, Li P, Chao L. Opposing effects of oxygen regulation on kallistatin expression: kallistatin as a novel mediator of oxygen-induced HIF-1-eNOS-NO pathway. *Oxid Med Cell Longev*. 2017;2017:5262958.
- Shen B, Chao L, Chao J. Pivotal role of JNK-dependent FOXO1 activation in downregulation of kallistatin expression by oxidative stress. *Am J Physiol Heart Circ Physiol*. 2010;298:H1048–H1054.
- Chao J, Schmaier A, Chen LM, Yang Z, Chao L. Kallistatin, a novel human tissue kallikrein inhibitor: levels in body fluids, blood cells, and tissues in health and disease. *J Lab Clin Med*. 1996;127:612–620.
- Pashkow FJ. Oxidative stress and inflammation in heart disease: do antioxidants have a role in treatment and/or prevention? *Int J Inflam*. 2011;2011:514623.
- Wolf WC, Harley RA, Sluce D, Chao L, Chao J. Localization and expression of tissue kallikrein and kallistatin in human blood vessels. *J Histochem Cytochem*. 1999;47:221–228.
- Lo Sasso G, Schlage WK, Boué S, Veljkovic E, Peitsch MC, Hoeng J. The Apoe (-/-) mouse model: a suitable model to study cardiovascular and respiratory diseases in the context of cigarette smoke exposure and harm reduction. *J Transl Med*. 2016;14:146.
- Chiu JJ, Chien S. Effects of disturbed flow on vascular endothelium: pathophysiological basis and clinical perspectives. *Physiol Rev*. 2011;91:327–387.
- Stein S, Matter CM. Protective roles of SIRT1 in atherosclerosis. *Cell Cycle*. 2011;10:640–647.
- Mattagajasingh I, Kim CS, Naqvi A, Yamamori T, Hoffman TA, Jung SB, DeRicco J, Kasuno K, Irani K. SIRT1 promotes endothelium dependent vascular relaxation by activating endothelial nitric oxide synthase. *Proc Natl Acad Sci USA*. 2007;104:14855–14860.
- Guo Y, Li P, Gao L, Zhang J, Yang Z, Bledsoe G, Chang E, Chao L, Chao J. Kallistatin reduces vascular senescence and aging by regulating microRNA-34a-SIRT1 pathway. *Aging Cell*. 2017;16:837–846.
- Chen Z, Peng IC, Cui X, Li YS, Chien S, Shyy JY. Shear stress, SIRT1 and vascular homeostasis. *Proc Natl Acad Sci USA*. 2010;107:10268–10273.
- Zhang QJ, Wang Z, Chen HZ, Zhou S, Zheng W, Liu G, Wei YS, Cai H, Liu DP, Liang CC. Endothelium-specific overexpression of class III deacetylase SIRT1 decreases atherosclerosis in apolipoprotein E-deficient mice. *Cardiovasc Res*. 2008;80:191–199.
- Alcendor RR, Gao S, Zhai P, Zablocki D, Holle E, Yu X, Tian B, Wagner T, Vatner SF, Sadoshima J. Sirt1 regulates aging and resistance to oxidative stress in the heart. *Circ Res*. 2007;100:1512–1521.
- Olmos Y, Sánchez-Gómez FJ, Wild B, García-Quintans N, Cabezu S, Lamas S, Monsalve M. Sirt1 regulation of antioxidant genes is dependent on the formation of a FoxO3a/PGC-1 α complex. *Antioxid Redox Signal*. 2013;19:1507–1521.